

**Correlation energies of the high-density spin-polarized electron gas to meV accuracy**Michele Ruggeri,<sup>1</sup> Pablo López Ríos,<sup>1,2</sup> and Ali Alavi<sup>1,3</sup><sup>1</sup>Max Planck Institute for Solid State Research, Heisenbergstrasse 1, 70569 Stuttgart, Germany<sup>2</sup>Theory of Condensed Matter Group, Cavendish Laboratory, J. J. Thomson Avenue, Cambridge CB3 0HE, United Kingdom<sup>3</sup>University Chemical Laboratory, Lensfield Road, Cambridge CB2 1EW, United Kingdom

(Received 13 April 2018; published 8 October 2018)

We present a combination of quantum Monte Carlo methods and a finite-size extrapolation framework with which we calculate the thermodynamic limit of the exact correlation energy of the polarized electron gas at high densities to meV accuracy,  $-40.44(5)$  and  $-31.70(4)$  mHa at  $r_s = 0.5$  and  $1$ , respectively. The fixed-node error is characterized and found to exceed 1 mHa, and we show that the magnitude of the correlation energy of the polarized electron gas is underestimated by up to 6 meV by the Perdew-Wang parametrization, for which we suggest improvements.

DOI: [10.1103/PhysRevB.98.161105](https://doi.org/10.1103/PhysRevB.98.161105)

The uniform (or homogeneous) electron gas (UEG) [1] is a system consisting of electrons in a neutralizing uniform background intended to model the behavior of electrons in metals [2]. This system is of crucial importance in understanding the nature of electronic correlations, and is of huge practical relevance since knowledge of the correlation energy of the UEG as a function of its homogeneous density can be used as a key ingredient in the description of the behavior of electrons in real systems [3–5].

Despite its seeming simplicity, the complex correlations caused by the long-ranged character of the Coulomb interaction require the use of explicit many-body methods to accurately characterize the UEG. The release-node diffusion Monte Carlo calculations of Ceperley and Alder (CA) [6] provided data connecting the analytic high-density [7,8] and low-density [9] limits of the correlation energy, and enabled the development of parametrizations over the entire density range [10–12] which are routinely used in density functional theory calculations.

The Perdew-Wang parametrization of the correlation energy of the UEG (PW92) [12] has become a cornerstone in the construction of density functionals over the past three decades. The PW92 form contains five parameters, of which two are determined from analytic high-density constraints and three by fitting to the CA data. More recently, a “density parameter interpolation” (DPI) parametrization was proposed [13–15] that is constructed by imposing four high-density and three low-density constraints on a seven-parameter functional form, thus requiring (almost) no quantum Monte Carlo input. In Fig. 1 we plot the PW92 and DPI parametrizations for the fully polarized electron gas, along with the asymptotes defined in Refs. [13–15], as a function of  $r_s$ , the radius of the sphere containing one electron on average divided by the Bohr radius. While the two parametrizations are in excellent agreement at low densities, they differ by  $\sim 20$  meV at densities relevant to systems with all-electron nuclei [16] and solids at high pressures. The cumulative effect of incurring these small errors in the parametrized correlation energy could result in a significant bias in

computed properties, including total and relative energy estimates.

In this Rapid Communication we use a combination of full configuration-interaction quantum Monte Carlo (FCIQMC) and fixed-node diffusion Monte Carlo (DMC) to compute the correlation energy of the fully spin-polarized three-dimensional UEG at  $r_s = 0.5$  and  $1$  to meV accuracy. Building upon existing knowledge of finite-size errors in DMC [17–20], we propose an extrapolation procedure which we find to be much more accurate than previous approaches. By extrapolating the fixed-node energy and the fixed-node error to the thermodynamic limit we obtain the exact correlation energies at  $r_s = 0.5$  and  $1$ . We are thus able to resolve the discrepancy between the values of the PW92 and DPI parametrizations at high densities, and we discuss ways to improve their accuracy.

We simulate finite systems of  $N$  same-spin electrons in a cubic simulation cell at fixed homogeneous densities using DMC and FCIQMC. Note that we report energies per electron and use Hartree atomic units ( $\hbar = m_e = |e| = 4\pi\epsilon_0 = 1$ ) throughout. Full details about the methodology and calculations are given in the Supplemental Material [21].

The variational Monte Carlo (VMC) [24–26] and fixed-node DMC methods [6,27–29] have been extensively used to study the UEG [30–34] using Slater-Jastrow trial wave functions, formed by the Hartree-Fock (HF) determinant multiplied by a Jastrow correlation factor [35,36], often in combination with backflow transformations [30–32,37,38]. While these wave functions are reasonably sophisticated, the energy obtained by the DMC method incurs a positive bias, referred to as the fixed-node error  $\epsilon_{\text{FN}}$ , caused by the restrictions imposed by the fixed-node approximation [6,39].

The FCIQMC method explicitly operates in the basis of antisymmetric Slater determinants, thus avoiding the need for a fixed-node approximation [40]. The initiator approximation [41] allows the efficient exploration of this vast Hilbert space, and has enabled the successful application of FCIQMC to systems of interest in quantum chemistry and condensed matter physics [42–47], including the unpolarized

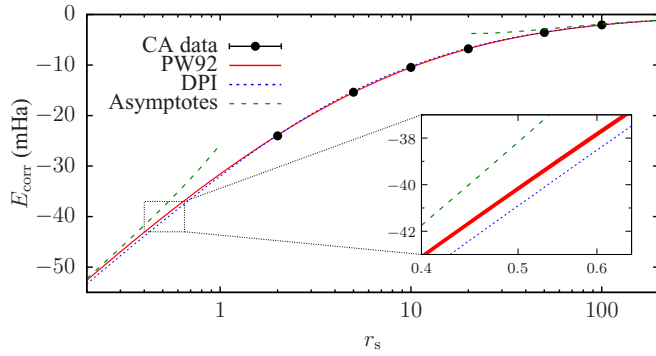


FIG. 1. Correlation energy of the polarized UEG as a function of  $r_s$ . Shown are the CA data [6], the PW92 parametrization [12], and the DPI parametrization [13–15]. The inset magnifies the region around  $r_s = 0.5$ . The width of the PW92 curve represents its statistical uncertainty.

UEG [48–51]. FCIQMC calculations use finite basis sets, and the infinite basis-set limit can be estimated by extrapolation, as is standard practice in quantum chemistry [52]. We find that the basis-set error for the polarized UEG is well described by a quadratic function of the inverse basis-set size [21], in contrast with the linear dependence found for the unpolarized UEG [48].

We assess the quality of our FCIQMC energies by comparison with VMC and DMC energies for increasingly accurate trial wave functions. We construct multideterminantal wave functions for the 19-electron gas at  $r_s = 1$  by truncating the FCIQMC wave function to the  $N_d$  leading determinants, with symmetry-equivalent determinants grouped together. The results, obtained using the CASINO code [53], are plotted in Fig. 2 against  $N_d$ .

The variational convergence of our VMC and DMC energies towards the FCIQMC energy is consistent with FCIQMC being exact for this system. The best backflow DMC energy is only 0.027(5) mHa higher than the FCIQMC energy, and is to our knowledge the most accurate DMC energy for this system reported to date.

The finite-size error in the energy of the UEG consists of a contribution which varies smoothly with  $N$  and a

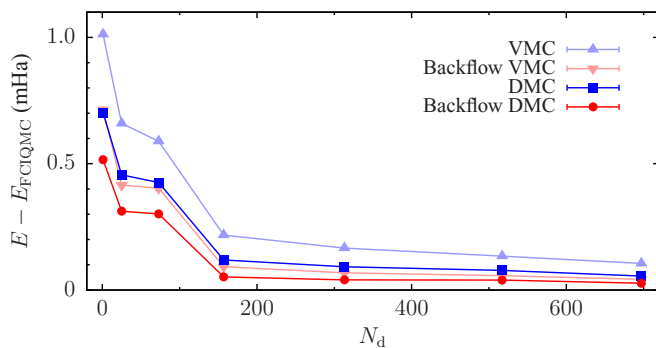


FIG. 2. VMC and DMC energies of the polarized 19-electron gas at  $r_s = 1$  (at  $\Gamma$ ) relative to FCIQMC, as a function of the number of determinants in the wave function, both without and with backflow transformations.

quasirandom contribution, which must be eliminated to enable a clean extrapolation of the smooth part. Twist averaging [17] substantially reduces quasirandom fluctuations by averaging over wave-vector offsets in the Brillouin zone. In DMC we sample the Brillouin zone randomly, while for our FCIQMC calculations we divide the Brillouin zone into regions of equal total momentum and run FCIQMC calculations in each of these regions [54], which we are able to characterize exactly [21]. In selected cases we perform the basis-set extrapolation in one region and use the extrapolation parameters for the others, which reduces the number of required FCIQMC calculations considerably [21]. In what follows we discuss twist averaged energies except when stated otherwise.

Quasirandom errors are further reduced by subtracting the finite-size error in the HF kinetic energy  $\Delta K(N) = K(N) - K(\infty)$  from the DMC total energy [6,19]. Additionally, we find that the residual quasirandom fluctuations are highly correlated with those in the HF exchange energy  $X(N)$ . The exchange energy is a particularly slowly varying function at large  $N$ , so subtracting  $X(N) - X(\infty)$  would complicate the extrapolation. However, Drummond *et al.* [19] found that the leading-order contribution to the finite-size error in  $X(N)$  for an electron gas is exactly  $h_2 N^{-2/3}$ , where  $h_2 = -\frac{3\epsilon_1}{16\pi} r_s^{-1}$  for the polarized UEG and  $\epsilon_1 = 5.674594959$  for simple cubic simulation cells [19,21]. We therefore obtain the thermodynamic limit by extrapolation of  $E_{\text{tot}}^{\text{FN}}(N) - \Delta K(N) - \Delta X(N)$ , where  $\Delta X(N) = X(N) - X(\infty) - h_2 N^{-2/3}$ . This is equivalent to extrapolating  $E_{\text{corr}}^{\text{FN}}(N) + h_2 N^{-2/3}$ , and in practice we work with the correlation energy directly.

We model the smooth part of the finite-size error as a polynomial in  $N^{-1/3}$ , in agreement with the form of the contributions found by Ref. [19], and we find that the use of the above treatment of quasirandom fluctuations enables the use of fairly high-order polynomials. Chiesa *et al.* [18] showed that the leading-order contribution to the finite-size error in the total DMC energy of an electronic system is  $t_3 N^{-1}$ , where  $t_3 = -\frac{\sqrt{3}}{2} r_s^{-3/2}$  for the polarized UEG. Since beyond-leading-order contributions to both  $\Delta K(N)$  and  $\Delta X(N)$  are proportional to  $N^{-4/3}$  [17,19], the DMC correlation energy satisfies

$$E_{\text{corr}}^{\text{FN}}(N) + h_2 N^{-2/3} - t_3 N^{-1} = c_0 + c_4 N^{-4/3} + c_5 N^{-5/3} + c_6 N^{-2} + \dots, \quad (1)$$

where  $\{c_n\}$  are density-dependent parameters.

We perform DMC calculations of the polarized UEG using the Slater-Jastrow wave function at system sizes  $15 \leq N \leq 515$  at  $r_s = 0.5$  and  $15 \leq N \leq 1021$  at  $r_s = 1$ , and we use Eq. (1) to obtain the thermodynamic limit of the fixed-node correlation energy, setting  $h_2$  and  $t_3$  to their analytic values and treating  $c_0$ ,  $c_4$ ,  $c_5$ , and  $c_6$  as fit parameters. We do not use backflow or multideterminants to avoid introducing wave-function optimization noise in our DMC energies. The magnitude of quasirandom fluctuations has been observed to decay as  $N^{-1}$  [17], so we use  $N^2$  as weights in our fits. In Fig. 3 we plot  $E_{\text{tot}}(N) - \Delta K(N) - \Delta X(N) - t_3 N^{-1}$  and our extrapolation (solid circles and solid line) at  $r_s = 0.5$  as a function of  $N^{-1}$ . These results numerically confirm the absence of additional contributions to Eq. (1) at order  $N^{-1}$  or slower.

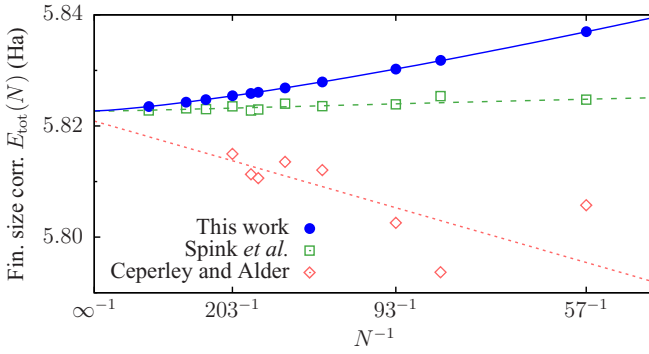


FIG. 3. Finite-size corrected fixed-node energies of the polarized UEG at  $r_s = 0.5$  as a function of  $N^{-1}$ . Our results correspond to the solid circles and the solid line. Data replicating the finite-size treatment of Ceperley and Alder [6] (open diamonds and dotted line) and Spink *et al.* [34] (open squares) are also plotted, along with an extrapolation of the latter using  $N^{-4/3}$  and  $N^{-5/3}$  terms.

In Fig. 3 we also compare our extrapolation with other approaches used in the literature. Ceperley and Alder [6] evaluated  $E_{\text{tot},\Gamma}(N) - \Delta K(N)$ , where  $E_{\text{tot},\Gamma}(N)$  is the total energy at  $\Gamma$ , at closed-shell system sizes in the range  $38 \leq N \leq 246$ , and used an extrapolation formula including a single  $N^{-1}$  term to obtain the thermodynamic limit. A reconstruction of this approach with our DMC data is represented in Fig. 3 (open diamonds and dotted line); we have used  $N^2$  as weights in the single-term fit. Remarkably, the choice of system sizes is such that the single-term extrapolation yields a nearly identical thermodynamic limit for  $\Gamma$ -point energies as for twist averaged energies, but the absence of higher-order terms in the extrapolation formula results in an underestimation of the total fixed-node energy by about 2 mHa. Higher-order contributions are less important at lower densities, and we conclude that the extrapolation carried out by Ceperley and Alder is very accurate at the densities for which they reported results.

The recent fixed-node DMC study of Spink *et al.* [34] can be regarded the current state of the art in the treatment of finite-size errors. Spink *et al.* approximate the thermodynamic limit of the total energy by the backflow DMC value of  $E_{\text{tot}}^{\text{FN}}(N) - \Delta K(N) - t_3 N^{-1} - T_4 N^{-4/3}$  at a single system size, where the last term is the next-to-leading-order contribution to the finite-size error in the DMC kinetic energy, with  $T_4 = \frac{\epsilon_3}{16\pi} r_s^{-2}$  for the polarized electron gas and  $\epsilon_3 = 21.049\,598\,45$  for simple cubic simulation cells [19,21]. Our reconstruction of this approach using our (nonbackflow) DMC data is presented in Fig. 3 (open squares). The quasirandom fluctuations obtained with this approach are small but still significant and, although the data extrapolate to the correct value, individual energy values in Fig. 3 overestimate the thermodynamic limit by up to over 2 mHa. Indeed, the thermodynamic limit of the backflow DMC correlation energy at  $r_s = 0.5$  reported by Spink *et al.*, obtained for a 118-electron system in a face-centered-cubic simulation cell, is 2.27(2) mHa above our estimate of the thermodynamic limit of the (nonbackflow) DMC correlation energy.

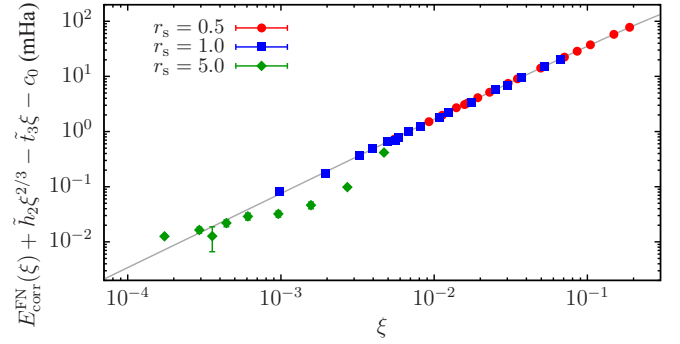


FIG. 4. Fixed-node correlation energies of the polarized UEG at  $r_s = 0.5, 1,$  and  $5$  relative to the thermodynamic limit as a function of  $\xi$ . The line represents a combined fit of the data at  $r_s = 0.5$  and  $1$  to Eq. (2), with density-dependent  $c_0$  and density-independent  $\tilde{c}_4, \tilde{c}_5,$  and  $\tilde{c}_6$  coefficients. The  $r_s = 5$  data demonstrate the breakdown of the approximate  $\xi$  dependence at low densities.

We turn our attention to the density dependence of Eq. (1), which we reexpress as

$$E_{\text{corr}}^{\text{FN}}(\xi) + \tilde{h}_2 \xi^{2/3} - \tilde{t}_3 \xi = c_0 + \tilde{c}_4 \xi^{4/3} + \tilde{c}_5 \xi^{5/3} + \tilde{c}_6 \xi^2 + \dots, \quad (2)$$

where  $\xi = r_s^{-3/2} N^{-1}$ . We find that assuming coefficients with tildes to be density independent, in line with leading-order extrapolation formulas proposed in the literature [55], incurs a negligible error at high densities. In Fig. 4 we plot  $E_{\text{corr}}^{\text{FN}}(\xi)$  and perform a combined fit of the data at  $r_s = 0.5$  and  $1$  to Eq. (2), which we find to fit the data very well [21]. We also plot fixed-node energies at  $r_s = 5$  to demonstrate the breakdown of this approximation at low densities.

We compute the exact energy of the system using FCIQMC at system sizes  $N = 15, 19,$  and  $27$  at  $r_s = 1$  and  $N = 15, 19, 27,$  and  $33$  at  $r_s = 0.5$ , and we evaluate the fixed-node error as the difference between the fixed-node and exact

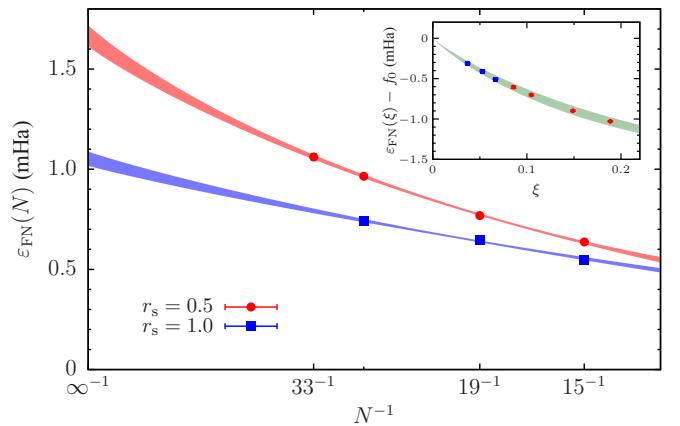


FIG. 5. Fixed-node error for the polarized UEG at  $r_s = 0.5$  and  $1$  as a function of  $N^{-1}$ . The curves are obtained by simultaneously fitting the data at both densities to Eq. (3) with density-dependent  $f_0$  and density-independent  $\tilde{f}_3$  and  $\tilde{f}_4$  coefficients. The linewidth represents the statistical uncertainty in the fit. The inset shows the combined fit against  $\xi$ .

TABLE I. Thermodynamic limit of the fixed-node correlation energy, of the fixed-node error, and of the exact correlation energy of the polarized UEG at  $r_s = 0.5$  and 1, in mHa. Also shown are values of the PW92 and DPI parametrizations, an unweighted PW92 fit to the CA data (uPW92), and a revised unweighted PW92 fit to the CA data and our results (rPW92).

|                               | $r_s = 0.5$ | $r_s = 1.0$ |
|-------------------------------|-------------|-------------|
| $E_{\text{corr}}^{\text{FN}}$ | -38.778(10) | -30.650(3)  |
| $\varepsilon_{\text{FN}}$     | 1.67(5)     | 1.05(4)     |
| $E_{\text{corr}}$             | -40.44(5)   | -31.70(4)   |
| PW92                          | -40.2(1)    | -31.6(1)    |
| DPI                           | -40.91      | -31.99      |
| uPW92                         | -40.4(5)    | -31.8(4)    |
| rPW92                         | -40.38(6)   | -31.77(8)   |

correlation energies. We find the fixed-node error to increase monotonically with system size [21].

Holzmann *et al.* [20] found that the use of backflow contributes to the finite-size error in the energy of the UEG at order  $N^{-1}$ . This has the subtle consequence that the coefficient of  $N^{-1}$  in the finite-size error of the exact energy must differ from  $t_3$ . We assume the fixed-node error to have the same asymptotic behavior as the backflow contribution to the energy, which is consistent with the observation of an approximate proportionality between these two quantities [30,56]. We expect  $\varepsilon_{\text{FN}}$  to vary less strongly with  $N$  than the fixed-node energy, and thus we model it using a lower-order expression. Under the assumption that, as  $E_{\text{corr}}^{\text{FN}}$ , the exact correlation energy is accurately represented at high densities by a function of  $\xi$ , we write

$$\varepsilon_{\text{FN}}(\xi) = f_0 + \tilde{f}_3 \xi + \tilde{f}_4 \xi^{4/3} + \dots, \quad (3)$$

where  $f_0$  is a density-dependent parameter and  $\tilde{f}_3$  and  $\tilde{f}_4$  are density-independent coefficients. We perform a combined fit of our data at  $r_s = 0.5$  and 1 to Eq. (3) to obtain the thermodynamic limit of the fixed-node error at both densities. In Fig. 5 we plot the fixed-node error and the resulting fit curves, and in the inset we show the same data as a function of  $\xi$ . The results obtained with this procedure are given in Table I and plotted in Fig. 6.

Before comparing our results with existing parametrizations, we note two problematic aspects of the PW92 fit. First, the statistical uncertainty of the CA data propagates to the parametrized correlation energies, which thus incur a random bias of magnitude proportional to the uncertainty, but this was ignored after fitting. We have calculated these propagated uncertainties, shown in Table I and Fig. 6. Second, the CA data were weighted by their inverse square uncertainty in the

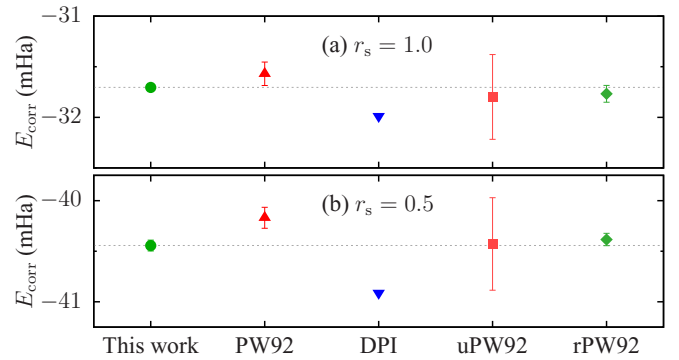


FIG. 6. Correlation energy of the polarized UEG at (a)  $r_s = 1$  and (b)  $r_s = 0.5$  from our calculations (dotted lines), and values of the PW92 and DPI parametrizations, our unweighted PW92 fit to the CA data (uPW92), and our revised unweighted PW92 fit to the CA data and our present results (rPW92).

PW92 fit (a “chi-square” fit), but these span over two orders of magnitude, and in effect the PW92 parametrization ignores the CA data for  $r_s \leq 10$ : Fitting the CA energies for  $r_s = 20, 50,$  and  $100$  to the PW92 form gives essentially identical results to the “chi-square” fit using all the data. In Table I and Fig. 6 we report values of an unweighted PW92 fit to the CA data (uPW92) and of an unweighted PW92 fit to the CA data and our present results (rPW92).

We find that the magnitude of the correlation energy is underestimated by the PW92 parametrization by about 3–6 meV, and overestimated by the DPI parametrization by 8–13 meV. The correlation energies obtained from the unweighted uPW92 fit have rather large uncertainties, but their expected values are more accurate than those from the weighted fit. Our revised rPW92 fit delivers the correct correlation energies at both densities with negligible bias and a factor of 5–10 smaller uncertainties than the uPW92 fit.

By construction, the accuracy of the DPI parametrization at finite densities depends exclusively on its functional form. Modifications to include more high-density constraints would be advisable in order to enable better agreement with our results. Alternatively, additional degrees of freedom could be used to fit parameters to quantum Monte Carlo data, which would be advantageous over our rPW92 fit since the DPI form has the correct analytic structure in the high- and low-density limits [13].

The authors would like to thank H. Luo, J. J. Shepherd, R. J. Needs, and M. Holzmann for useful discussions. Financial support and computational resources have been provided by the Max-Planck-Gesellschaft.

- [1] P.-F. Loos and P. M. W. Gill, The uniform electron gas, *Wiley Interdiscip. Rev.: Comput. Mol. Sci.* **6**, 410 (2016).  
 [2] S. Huotari, J. A. Soininen, T. Pylkkänen, K. Hämäläinen, A. Issolah, A. Titov, J. McMinis, J. Kim, K. Esler, D. M. Ceperley, M. Holzmann, and V. Olevano, Momentum Distribution and

- Renormalization Factor in Sodium and the Electron Gas, *Phys. Rev. Lett.* **105**, 086403 (2010).  
 [3] E. Wigner, Effects of the electron interaction on the energy levels of electrons in metals, *Trans. Faraday Soc.* **34**, 678 (1938).

- [4] P. Hohenberg and W. Kohn, Inhomogeneous electron gas, *Phys. Rev.* **136**, B864 (1964).
- [5] W. Kohn and L. J. Sham, Self-consistent equations including exchange and correlation effects, *Phys. Rev.* **140**, A1133 (1965).
- [6] D. M. Ceperley and B. J. Alder, Ground State of the Electron Gas by a Stochastic Method, *Phys. Rev. Lett.* **45**, 566 (1980).
- [7] M. Gell-Mann and K. A. Brueckner, Correlation energy of an electron gas at high density, *Phys. Rev.* **106**, 364 (1957).
- [8] G. G. Hoffman, Correlation energy of a spin-polarized electron gas at high density, *Phys. Rev. B* **45**, 8730 (1992).
- [9] W. J. Carr, Jr., Energy, specific heat, and magnetic properties of the low-density electron gas, *Phys. Rev.* **122**, 1437 (1961).
- [10] S. H. Vosko, L. Wilk, and M. Nusair, Accurate spin-dependent electron liquid correlation energies for local spin density calculations: A critical analysis, *Can. J. Phys.* **58**, 1200 (1980).
- [11] J. P. Perdew and A. Zunger, Self-interaction correction to density-functional approximations for many-electron systems, *Phys. Rev. B* **23**, 5048 (1981).
- [12] J. P. Perdew and Y. Wang, Accurate and simple analytic representation of the electron-gas correlation energy, *Phys. Rev. B* **45**, 13244 (1992).
- [13] J. Sun, J. P. Perdew, and M. Seidl, Correlation energy of the uniform electron gas from an interpolation between high- and low-density limits, *Phys. Rev. B* **81**, 085123 (2010).
- [14] P.-F. Loos and P. M. W. Gill, Correlation energy of the spin-polarized uniform electron gas at high density, *Phys. Rev. B* **84**, 033103 (2011).
- [15] P. Bhattarai, A. Patra, C. Shahi, and J. P. Perdew, How accurate are the parametrized correlation energies of the uniform electron gas? *Phys. Rev. B* **97**, 195128 (2018).
- [16] A. Zupan, K. Burke, M. Ernzerhof, and J. P. Perdew, Distributions and averages of electron density parameters: Explaining the effects of gradient corrections, *J. Chem. Phys.* **106**, 10184 (1997).
- [17] C. Lin, F. H. Zong, and D. M. Ceperley, Twist-averaged boundary conditions in continuum quantum Monte Carlo algorithms, *Phys. Rev. E* **64**, 016702 (2001).
- [18] S. Chiesa, D. M. Ceperley, R. M. Martin, and M. Holzmann, Finite-Size Error in Many-Body Simulations with Long-Range Interactions, *Phys. Rev. Lett.* **97**, 076404 (2006).
- [19] N. D. Drummond, R. J. Needs, A. Sorouri, and W. M. C. Foulkes, Finite-size errors in continuum quantum Monte Carlo calculations, *Phys. Rev. B* **78**, 125106 (2008).
- [20] M. Holzmann, R. C. Clay, III, M. A. Morales, N. M. Tubman, D. M. Ceperley, and C. Pierleoni, Theory of finite size effects for electronic quantum Monte Carlo calculations of liquids and solids, *Phys. Rev. B* **94**, 035126 (2016).
- [21] See Supplemental Material at <http://link.aps.org/supplemental/10.1103/PhysRevB.98.161105> for details of the system and methodology, including twist averaging, Brillouin zone division, trial wave functions, finite-size errors, and additional results, which includes Refs. [22,23].
- [22] P. P. Ewald, Die Berechnung optischer und elektrostatischer Gitterpotentiale, *Ann. Phys.* **369**, 253 (1921).
- [23] T. Kato, On the eigenfunctions of many-particle systems in quantum mechanics, *Commun. Pure Appl. Math.* **10**, 151 (1957).
- [24] W. L. McMillan, Ground state of liquid He<sup>4</sup>, *Phys. Rev.* **138**, A442 (1965).
- [25] J. Toulouse and C. J. Umrigar, Optimization of quantum Monte Carlo wave functions by energy minimization, *J. Chem. Phys.* **126**, 084102 (2007).
- [26] C. J. Umrigar, J. Toulouse, C. Filippi, S. Sorella, and R. G. Hennig, Alleviation of the Fermion-Sign Problem by Optimization of Many-Body Wave Functions, *Phys. Rev. Lett.* **98**, 110201 (2007).
- [27] W. M. C. Foulkes, L. Mitas, R. J. Needs, and G. Rajagopal, Quantum Monte Carlo simulations of solids, *Rev. Mod. Phys.* **73**, 33 (2001).
- [28] C. J. Umrigar, M. P. Nightingale, and K. J. Runge, A diffusion Monte Carlo algorithm with very small time-step errors, *J. Chem. Phys.* **99**, 2865 (1993).
- [29] A. Zen, S. Sorella, M. J. Gillan, A. Michaelides, and D. Alfè, Boosting the accuracy and speed of quantum Monte Carlo: Size consistency and time step, *Phys. Rev. B* **93**, 241118(R) (2016).
- [30] Y. Kwon, D. M. Ceperley, and R. M. Martin, Effects of backflow correlation in the three-dimensional electron gas: Quantum Monte Carlo study, *Phys. Rev. B* **58**, 6800 (1998).
- [31] M. Holzmann, D. M. Ceperley, C. Pierleoni, and K. Esler, Backflow correlations for the electron gas and metallic hydrogen, *Phys. Rev. E* **68**, 046707 (2003).
- [32] P. López Ríos, A. Ma, N. D. Drummond, M. D. Towler, and R. J. Needs, Inhomogeneous backflow transformations in quantum Monte Carlo calculations, *Phys. Rev. E* **74**, 066701 (2006).
- [33] I. G. Gurtubay, R. Gaudoin, and J. M. Pitarke, Benchmark quantum Monte Carlo calculations of the ground-state kinetic, interaction and total energy of the three-dimensional electron gas, *J. Phys.: Condens. Matter* **22**, 065501 (2010).
- [34] G. G. Spink, N. D. Drummond, and R. J. Needs, Quantum Monte Carlo study of the three-dimensional spin-polarized homogeneous electron gas, *Phys. Rev. B* **88**, 085121 (2013).
- [35] N. D. Drummond, M. D. Towler, and R. J. Needs, Jastrow correlation factor for atoms, molecules, and solids, *Phys. Rev. B* **70**, 235119 (2004).
- [36] P. López Ríos, P. Seth, N. D. Drummond, and R. J. Needs, Framework for constructing generic Jastrow correlation factors, *Phys. Rev. E* **86**, 036703 (2012).
- [37] V. R. Pandharipande and N. Itoh, Effective mass of <sup>3</sup>He in liquid <sup>4</sup>He, *Phys. Rev. A* **8**, 2564 (1973).
- [38] K. E. Schmidt and V. R. Pandharipande, New variational wave function for liquid <sup>3</sup>He, *Phys. Rev. B* **19**, 2504 (1979).
- [39] J. B. Anderson, Quantum chemistry by random walk. H <sup>2</sup>P, H<sub>3</sub><sup>+</sup>D<sub>3h</sub><sup>1</sup>A<sub>1</sub><sup>+</sup>, H<sub>2</sub>3Σ<sub>u</sub><sup>+</sup>, H<sub>4</sub><sup>1</sup>Σ<sub>g</sub><sup>+</sup>, Be <sup>1</sup>S, *J. Chem. Phys.* **65**, 4121 (1976).
- [40] G. H. Booth, A. J. W. Thom, and A. Alavi, Fermion Monte Carlo without fixed nodes: A game of life, death, and annihilation in Slater determinant space, *J. Chem. Phys.* **131**, 054106 (2009).
- [41] D. Cleland, G. H. Booth, and A. Alavi, Survival of the fittest: Accelerating convergence in full configuration-interaction quantum Monte Carlo, *J. Chem. Phys.* **132**, 041103 (2010).
- [42] D. Cleland, G. H. Booth, C. Overy, and A. Alavi, Taming the first-row diatomics: A full configuration interaction quantum Monte Carlo study, *J. Chem. Theory Comput.* **8**, 4138 (2012).
- [43] J. A. F. Kersten, G. H. Booth, and A. Alavi, Assessment of multireference approaches to explicitly correlated full configuration

- interaction quantum Monte Carlo, *J. Chem. Phys.* **145**, 054117 (2016).
- [44] L. R. Schwarz, G. H. Booth, and A. Alavi, Insights into the structure of many-electron wave functions of Mott-insulating antiferromagnets: The three-band Hubbard model in full configuration interaction quantum Monte Carlo, *Phys. Rev. B* **91**, 045139 (2015).
- [45] G. H. Booth and A. Alavi, Approaching chemical accuracy using full configuration-interaction quantum Monte Carlo: A study of ionization potentials, *J. Chem. Phys.* **132**, 174104 (2010).
- [46] D. Cleland, G. H. Booth, and A. Alavi, A study of electron affinities using the initiator approach to full configuration interaction quantum Monte Carlo, *J. Chem. Phys.* **134**, 024112 (2011).
- [47] G. H. Booth, D. Cleland, A. J. W. Thom, and A. Alavi, Breaking the carbon dimer: The challenges of multiple bond dissociation with full configuration interaction quantum Monte Carlo methods, *J. Chem. Phys.* **135**, 084104 (2011).
- [48] J. J. Shepherd, G. H. Booth, and A. Alavi, Investigation of the full configuration interaction quantum Monte Carlo method using homogeneous electron gas models, *J. Chem. Phys.* **136**, 244101 (2012).
- [49] J. J. Shepherd, G. H. Booth, A. Grüneis, and A. Alavi, Full configuration interaction perspective on the homogeneous electron gas, *Phys. Rev. B* **85**, 081103(R) (2012).
- [50] H. Luo and A. Alavi, Combining the transcorrelated method with full configuration interaction quantum Monte Carlo: Application to the homogeneous electron gas, *J. Chem. Theory Comput.* **14**, 1403 (2018).
- [51] V. A. Neufeld and A. J. W. Thom, A study of the dense uniform electron gas with high orders of coupled cluster, *J. Chem. Phys.* **147**, 194105 (2017).
- [52] T. Helgaker, P. Jørgensen, and J. Olsen, *Molecular Electronic-Structure Theory* (Wiley, Chichester, 2000).
- [53] R. J. Needs, M. D. Towler, N. D. Drummond, and P. López Ríos, Continuum variational and diffusion quantum Monte Carlo calculations, *J. Phys.: Condens. Matter* **22**, 023201 (2010).
- [54] J. J. Shepherd, A quantum chemical perspective on the homogeneous electron gas, Ph.D. thesis, University of Cambridge, (2013).
- [55] D. M. Ceperley, Ground state of the fermion one-component plasma: A Monte Carlo study in two and three dimensions, *Phys. Rev. B* **18**, 3126 (1978).
- [56] P. Seth, P. López Ríos, and R. J. Needs, Quantum Monte Carlo study of the first-row atoms and ions, *J. Chem. Phys.* **134**, 084105 (2011).